VOL. 16, NO. 10, MAY 2021 ISSN 1819-6608
ARPN Journal of Engineering and Applied Sciences
©2006-2021 Asian Research Publishing Network (ARPN). All rights reserved.
www.arpnjournals.com

SCHEDULING AND RESOURCE ALLOCATION FOR FILTER BANK MULTICARRIER MILLIMETER-WAVE DEVICE-TO-DEVICE COMMUNICATION

Filbert Onkundi Ombongi[1], Heywood Ouma Absaloms[2] and Philip Langat Kibet[3]
[1]Pan African University Institute for Basic Sciences, Technology and Innovation, Kenya
[2]Department of Electrical and Information Engineering, University of Nairobi, Kenya
[3]Department of Telecommunication and Information Engineering, Jomo Kenyatta University of Agriculture and Technology, Kenya
E-Mail: onkundifilo12@gmail.com

ABSTRACT

The deployment of Device-to-Device (D2D) communication in the millimeter-wave (mm-wave) band has shown the potential of significantly improving performance in terms of capacity, energy efficiency, and transmission latency. The high mm-wave frequencies offer a broader spectrum, compared to the current cellular networks, which enhances the deployment of highly directional antenna arrays to reduce interference problems. However, deployment of D2D communication in the mm-wave band is faced with a challenge of signal blockage by obstacles. In addition, if users are subjected to some mobility, there will be beam misalignments between the transmitter and the receiver and frequent monitoring and handovers. In dense D2D communication in the mm-wave band, there is interference between the multiple D2D devices. All these cases increase interference in the mm-wave D2D communication network. Therefore, an effective mechanism needs to be developed to reduce this interference to maximize the D2D user capacity by allocating resources effectively. The paper aims to formulate a joint uplink scheduling and resource allocation scheme to maximize the user capacity in a MIMO-enabled mm-wave D2D network with user mobility. The developed mm-wave D2D model integrates Filter Bank Multicarrier/Offset Quadrature Amplitude Modulation (FBMC/OQAM), MIMO Space-Time Coding (STC) and Spatial Multiplexing (SM) which are implemented separately and their performance compared. The developed mm-wave D2D model is simulated and its results compared with the conventional Orthogonal Frequency Division Multiplexing (OFDM) scheme. The results indicate that the FBMC/OQAM outperformed OFDM by an average factor of 2.03 times for I=64, LOS, 2.53 for I=64, NLOS, 2.08 for I=256, LOS, 2.45 for I=256, NLOS, 2.08 for STC, LOS and 2.30 for STC, NLOS.

Keywords: mm-wave, device-to-device, FBMC/OQAM, OFDM, scheduling.

INTRODUCTION

The Fifth Generation (5G) wireless technology can support different bandwidth-intensive services in the millimeter-wave band. The services include augmented and virtual reality, video streaming, online gaming, social networking, and multimedia file transfers. The mobile users in 5G are expected to offer better quality in high traffic, high density, and high-speed network scenarios which can be experienced in urban residential places, offices, social halls, railway stations, and stadiums. These network scenarios require instant connectivity at a lower latency and multi-giga-bits per second data rate. These objectives can only be realized by emerging technologies such as heterogeneous networks (HetNets), device-to-device communications, base stations with a massive number of antennas, and high-frequency communication as discussed in [1]. However, the mm-wave signals are prone to higher path loss compared to the current cellular communication signals. In addition, mm-wave communication is highly susceptible to blockage against solid barriers, such as buildings, human bodies, due to its short wavelengths [2, 3]. The potential of millimeter-wave being used for cellular communication network design has been shown in [4]. The D2D communication can be deployed in the mm-wave band and operate in three modes i.e. dedicated mode, reuse mode, and the cellular mode [5]. In [6] and [7], it has been shown that the high path loss problem in mm-wave can be reduced by employing beamforming technology which provides high directional gains in mm-wave communication.

The use of highly directional antennas and the availability of large bandwidth in the mm-wave band can offer a high data rate throughput and reduce the outage probability. However, this high data rate throughput can be degraded by user device mobility which may cause beam misalignment between the transmitter and receiver. This would give rise to unstable channel conditions. Therefore, to provide higher throughput for the mobile user devices, there is a need to develop a scheduling and resource allocation (power) algorithm for D2D links in the millimeter-wave band by considering the mobility of D2D devices operating in cellular mode and mm-wave channel conditions. The D2D devices communicate through Base Station (BS) when operating under the cellular mode.

The 5G new radio is characterized by signal waveform technologies such as OFDM and FBMC/OQAM. The frequencies of the subcarriers in OFDM are selected such that the orthogonality property is maintained between the subcarriers to mitigate the effect of cross-talk between inter-carrier guard bands and sub-channels. The cyclic prefix is added at the start of the OFDM waveform to overcome the problem of synchronizing time and frequency at the receiver. A set of high spectral selectivity filters are applied in

©2006-2021 Asian Research Publishing Network (ARPN). All rights reserved.

FBMC/OQAM to minimize cross-talk in place of a cyclic prefix. The potential of FBMC/OQAM working well in practical communication systems has been demonstrated in some recent studies for content delivery in next-generation 5G systems with promising results obtained. In [8], the FBMC/OQAM which has been proposed as a signal waveform technique by 3GPP for 5G was applied in the second generation Digital Video Broadcasting Terrestrial (DVB-T2 network and its results compared with the cyclic prefix OFDM. The performance was analyzed based on a bit error rate performance metric. The FBMC/OQAM has also been applied in satellite communication networks in related works of [9] and [10] by considering some of the 5G requirements. The performance comparison between FBMC/OQAM and conventional OFDM was based on total degradation with varying values of output back off and spectral efficiency. The result showed that the FBMC based scheme performed better than OFDM by 12.5%. In a similar manner the FBMC/OQAM can be applied to D2D communication networks to achieve higher data rates as shown in [11], which has implemented the D2D communication in the microwave band.

The current study has chosen the FBMC/OQAM application to D2D communication networks since it can reduce the complexity of the resource allocation techniques and offers better spectral localization in the frequency domain to minimize inter-user interference. In addition, the FBMC scheme can minimize the out of band leakage power, does not contain a cyclic prefix which is used in OFDM and reduced sensitivity to frequency variations as shown in [12].

In this paper, the performance of D2D users communicating in cellular mode is evaluated by formulating a dynamic scheduling and resource allocation mechanism with user mobility in a single cell. The formulated scheduling and power allocation mechanism maximizesthe capacity by applying the best channel quality indicator (BCQI) scheduling algorithm in a D2D-enabled millimeter-wave multicarrier communication network. In addition, the multicarrier communication applied is FBMC/OQAM and the dynamic nature of the D2D users is considered by incorporating the mobility of the users in an outdoor environment. The FBMC/OQAM modulation scheme performance is then compared with OFDM which is used in the current cellular communication networks. The main contribution of this study includes;

a) Formulation of a joint scheduling and resource allocation mechanism in an FBMC/OQAM based D2D communication network with user mobility.
b) Integrate MIMO space-time coding and spatial multiplexing to the developed FBMC based mm-wave D2D model and analyzing the capacity attained.
c) Demonstrate that the FBMC/OQAM based resource allocation reduces interference which improves the user capacity compared to the conventional OFDM based communication

The paper is organized as; Section 1 gives the introduction, Section 2 presents the related work. Section 3 discusses the system model and problem formulation and modeling, Section 4 describes the user mobility and blockage models, Section 5 discusses the multicarrier communication scheme, Section 6 describes the mmwave channel model, Section 7 presents simulation and performance evaluation, Section 8 gives the conclusion of the study.

RELATED WORK

In the microwave band, scheduling and resource allocation problem has been studied for FBMC/OQAM and OFDM multicarrier modulation formats. In [13], a cross-layer downlink scheduling and resource allocation process was proposed. The greedy scheduling and resource allocation algorithm was based on the physical layer and queueing model method at the data link control. The performance parameters such as delay, fairness, and service coverage were considered at 2.1 GHz microwave band to analyze FBMC/OQAM and OFDM. This study was extended in [14] by integrating dynamic programming based cross-layer scheduling and resource allocation scheme with FBMC/OQAM for higher spectral efficiency compared to OFDM. However, both studies did not incorporate the features of mm-wave communication such as path loss and shadowing effects. In addition, the served users by the base station in the downlink were not subjected to any mobility to evaluate its effect on the developed scheme.

An SINR-aware optimization problem was formulated in [15] to optimize the outage and bit error probabilities and the network capacity. The optimization function which was jointly doing mode selection, scheduling, and resource allocation was solved by applying the greedy heuristic algorithm for dedicated and reuse mode. However, this study did not incorporate the user mobility model, mm-wave path loss model, and multicarrier modulation in the LTE PHY layer signal processing.

In [16], a clustered IoT application based on D2D communication was implemented by considering OFDM, FBMC, Generalized Frequency Division Multiplexing (GFDM), and universal filtered multicarrier modulation schemes. The study was done by varying the size of the cell and cluster, transmit power of D2D devices, timing, and carrier frequency offset. In [17], a potential game-based distributed iterative power allocation algorithm was considered for D2D communications coexisting with OFDMA cellular user equipment to optimize the sum-rate. The afore-mentioned scheme has been extended to mm-wave cellular communication networks based on resource allocation, scheduling, and interference management either jointly or separately in a static or dynamic environment. In [18], an outage probability reduction problem was analyzed by proposing a power allocation and scheduling framework in an outdoor environment with user mobility. The outage probability optimization function was formulated with a goal of optimizing the aggregate number of time slots with a guarantee of throughput

©2006-2021 Asian Research Publishing Network (ARPN). All rights reserved.

requirements for the scheduled users. However, this study did not consider the effect of integrating the scheduling scheme and power allocation mechanism with multicarrier modulation schemes which have the potential of further improving the throughput of users in mm-wave communication. In [19], a mixed-integer nonlinear programming joint scheduling and radio resource optimization problem was studied in mm-wave heterogeneous networks in a scenario of dense mm-wave small cells in a conventional macrocell. The mm-wave small cells were operating in time division duplex mode and shared resources with the backhaul and access links. However, this study did not consider the effect of mobility for users in the mm-wave small cells. In [20], a greedy, round-robin, and proportional fair scheduling algorithms were studied for the effective allocation of resources in the physical layer design of a 5G network to minimize interference. The study incorporated coded generalized frequency division multiplexing (GFDM) for data rate improvement. The performance of the developed model was analyzed based on the throughput (with varying number of cellular users), symbol error rate (with varying SINR), path loss (with varying distance of the user from the base station and mm-wave carrier frequency) and energy efficiency for varying spectrum efficiency. In [21], a scheduling scheme was formulated that was based on time and space division to perform time-slot allocation to maximize the system data rate for each time slot. The study applied a resource allocation algorithm based on vertex coloring by considering both the main lobe and side lobe gains to reduce the side-lobe interference. The concurrent communication scenario was also taken into consideration in the developed model. However, this multicarrier based on GFDM did not consider the power allocation problem and the effect of the mobility of the user devices. The formulated scheduling and resource allocation functions in these studies are mostly nonlinear and the solution techniques tend to have high computation complexity. The complexity is further increased if the scheduling and resource allocation schemes incorporate user mobility. Therefore, there is need to apply the enabling technologies and mathematical solution techniques so they can reduce complexity and give optimal results.

The present work differs from the aforementioned studies which have been carried in either the microwave or mm-wave band. This study focusses on a joint scheduling and power allocation optimization problem for the FBMC/OQAM based mm-wave D2D communication with user mobility. In addition, the FBMC/OQAM based D2D communication model incorporates MIMO space-time coding and spatial multiplexing. The developed mm-wave D2D model can be applied in practical systems for video streaming applications [22] and digital TV broadcasting [10] by modifying the LTE PHY layer to minimize the inter-user interference and maximizing the data rate.

MODELING AND PROBLEM FORMULATION

This section gives the network layout and how the users are generated and distributed within the cell. Then, a scheduling and power allocation optimization problem is formulated to maximize the sum rate.

A. System Model

Consider a mm-wave multicarrier communication network with a transmitter and receiver, with a set of D2D users $U = \{1, \dots, N\}$ randomly distributed in a single cell by a Poisson Point Process (PPP) with a density, λ. The study assumed a dual-mode BS which operates in the microwave and mm-wave bands [23] and controls all the D2D user communication in the uplink and downlink. This enables the mitigation of D2D users and cellular users' interference as D2D communication is dedicated to the mm-wave band. The BS is responsible for allocating resources in uplink and downlink D2D communications. The peak transmission power of each device-to-device communication user device can be denoted as, P_t and the set of Resource Blocks (RBs) $\mathbb{B} = \{1, \dots, M\}$ serves the D2D users in the network. The D2D user devices are mobile and are allowed to enter and exit the network. The scheduling and resource allocation is assumed to be formulated for uplink data flow from the D2D transmitter (D_T) device to the BS. The Poisson distribution is used to model random D2D user distribution in the cell. The probability of the Poisson distribution is given as;

$$p(x, y) = \frac{e^{-\lambda}\lambda^{x}}{x!} \quad for\ x = 0,1,2 \tag{1}$$

where λ is the average number of users entering the cell in a given time.

The transmission process between an active D2D transmitter device and the dual-band BS is arranged in time-frequency RBs. Each RB takes a time and frequency slot for N_f subcarriers with the number of resource elements contained in each of them. The FBMC/OQAM symbols with a symbol period T_s are contained in each RB. The number of FBMC/OQAM symbols for each time slot is $N_s$which have a symbol period T_s and the subcarrier bandwidth is taken as $\Delta f = \frac{1}{T_s}$. The time slot size for FBMC/OQAM symbol is given as;

$$T_s = N_s \times T_p \tag{2}$$

Each resource block for the FBMC/OQAM communication system contains in the frequency domain a set of N_f adjacent subcarriers and a transmit time period of one transmit time interval (TTI). The study considers the performance of different power delay profiles for FBMC/OQAM and is consistent over all the available subcarriers. The scheduling and resource allocation processes are assumed to occur from the start of the transmission time interval.

B. Formulation of a Joint Scheduling and Power Allocation Optimization Problem

The D2D transmitter device has N_T transmit antennas and N_R receive antennas. Let g_{ij} be the link gain for D2D transmitter (D_T) device i ($i \in U$) communication

©2006-2021 Asian Research Publishing Network (ARPN). All rights reserved.

to a dual-band base station (BS) on the j[th] RB. The D2D communication in cellular mode utilizes the dedicated millimeter-wave band in this base station in an outdoor environment. The Friis transmission equation in [24] is used to model the link gain as in (3);

$$g_{ij} = \frac{g_i^T g_i^R \lambda^2}{16\pi^2 (d_i/d_o)^\alpha} \quad (3)$$

where g_i^T, g_i^R are the transmit antenna gain and receive antenna gain from user device i to BS respectively; d_i is the distance from D_T, i to BS at the j^{th} RB; d_o is the reference distance and α is the user device-to-BS link loss parameter. The SINR of user device i on the j^{th} RB can be determined as in (4);

$$\gamma_{ij} = \frac{p_{ij} g_{ij}}{\sum_{k \in U, k \neq i} p_{kj} g_{kj} + N_o} \quad (4)$$

where p_{ij} is the transmission power from D_T, i in the j^{th} RB, N_o is noise power, g_{ij} is the link gain from user device i to BS transmission at the j^{th} RB, g_{kj} is the link gain for transmission from other D_T devices. The achievable data rate for D_T, i can be computed by (5);

$$r_{ij} = W \log_2(1 + \gamma_{ij}) \quad (5)$$

Then the total capacity of the network is given by (6);

$$R_{ij} = \sum_{i=1}^{N} r_{ij} \quad (6)$$

A scheduling parameter is introduced that shows if the resource allocation has been done or not such that $x_{ij} = 1$, if D_T, i has been allocated RB, j($j \in \mathbb{B}$), and zero otherwise. The best channel quality indicator (BCQI) scheduler solves the radio resource allocation function for data rate maximization subject to some constraints. The data rate maximization function can then be expressed as in (7);

$$\max_{\mathrm{p}} \sum_{\mathrm{i}=1}^{\mathrm{N}} \sum_{\mathrm{b}=1}^{\mathrm{M}} \mathrm{x_{ij}} \mathrm{R_{ij}}$$

subject to

$$\begin{aligned} &\mathrm{C1}: \sum_{\mathrm{b}=1}^{\mathrm{B}} \mathrm{p_{ij}} \leq \mathrm{p_{max}}, \forall\, \mathrm{i} \in \mathrm{U} \\ &\mathrm{C2}: \mathrm{R_{ij}} \geq \mathrm{R_i^{min}}, \forall\, \mathrm{i} \in \mathrm{U} \\ &\mathrm{C3}: \mathrm{p_{ij}} \geq 0, \forall\, \mathrm{i} \in \mathrm{U}, \mathrm{j} \in \mathbb{B} \\ &\mathrm{C4}: \sum_{\mathrm{i}=1}^{\mathrm{N}} \mathrm{x_{ij}} \leq 1, \forall \mathrm{j} \in \mathbb{B} \end{aligned} \quad (7)$$

The formulated optimization function is a nonlinear mixed-integer programming function. The constraint C_1 shows the maximum transmit power requirement from user device i to the BS, C_2 ensures the minimum data rate requirement, C_3 governs the range of transmit power, and C_4 ensures only the available RBs are assigned to users. The constraints have a limitation on the throughput attained and the transmission power. The objective function is a concave function due to its fractional form.

C. Problem Solution

The solution to this type of optimization function is determined through the application of convex optimization properties. This can involve the application of nonlinear fractional programming theory to perform a fractional objective transformation to a convex optimization function [25]. The Lagrangian associated with the sum-rate optimization objective function is given as in (8);

$$\mathcal{L}(p_{ij}, \beta_i, \rho_i) = R_i(p_{ij}) - \beta_i\{R_i(p_{ij}) - R_i^{min}\} - \rho_i\left(\sum_{b=1}^{M} p_{ij} - p_{max}\right) \quad (8)$$

where β_i and ρ_i are the dual variables for C_1 and C_2 constraints respectively; R_i^{min} is the minimum data rate threshold, $R_i(p_{ij})$ is the achievable sum-rate which is a function of power allocated to RBs. The equivalent Lagrange dual optimization problem becomes;

$$\min_{(\beta_i \geq 0, \rho_i \geq 0)} \max_{(p_{ij})} \mathcal{L}(p_{ij}, \beta_i, \rho_i) \quad (9)$$

The optimization function which is now a dual function can be split into two optimization functions: one solves the power allocation maximization function to determine the optimal value of the transmitted power. The other part solves the original Lagrange dual optimization function to determine the values of the Lagrange multipliers which is a minimization function. The optimal transmit power can be determined by the Lagrange dual decomposition and the Karush Kuhn Tucker conditions. For any given value of β_i and ρ_i, the solution of the optimal value of transmit power is given by (10);

$$p_{ij} = \left[\frac{(1+\beta_i)\log_2 e}{\rho_i} - \frac{\sum_{k \in U, k \neq i} p_{kj} g_{kj} + N_o}{g_{ij}}\right]^+ \quad (10)$$

where, $[x]^+ = \max\{0, x\}$. The equation shows a water-filling power allocation algorithm to optimize the transmit power allocation and minimize inter-user interference since it reduces water level. The first and second-order partial derivatives are determined by $\mathcal{L}(p_{ij}, \beta_i, \rho_i)$ with respect to p_{ij} as $\frac{\partial \mathcal{L}(p_{ij}, \beta_i, \rho_i)}{\partial p_{ij}}$ and $\frac{\partial^2 \mathcal{L}(p_{ij}, \beta_i, \rho_i)}{\partial p_{ij}^2}$ respectively. The Newton positive decreasing steps $\mu_{i,\beta}(\tau)$ and $\mu_{i,\rho}(\tau)$ are determined by getting the ratio of the first derivative and second derivative of the Lagrangian function given by (11) as [26];

$$\mu_i(\tau) = \frac{\partial \mathcal{L}(p_{ij}, \beta_i, \rho_i)/\partial p_{ij}}{\partial^2 \mathcal{L}(p_{ij}, \beta_i, \rho_i)/\partial p_{ij}^2} \quad (11)$$

The Newton decrement which is often used as the stopping criteria is determined by (12) as;

©2006-2021 Asian Research Publishing Network (ARPN). All rights reserved.

$$\Theta = \frac{\left(\partial \mathcal{L}(p_{ij},\beta_i,\rho_i)/\partial p_{ij}\right)^2}{\partial^2 \mathcal{L}(p_{ij},\beta_i,\rho_i)/\partial p_{ij}^2} \quad (12)$$

This shows the optimal solution of (8) can be found from Newton's method [26]. Then, applying the sub-gradient method and positive Newton steps, the dual variables in (8) can be updated by (13);

$$\beta_i(\tau+1) = \left[\beta_i(\tau) - \mu_{i,\beta}(\tau)R_i(p_{ij}) - R_i^{min}\right]^+ \quad (3)$$

$$\rho_i(\tau+1) = \left[\rho_i(\tau) - \mu_{i,\rho}(\tau)\sum_{b=1}^{B} p_{ij} - p_{max}\right]^+ \quad (4)$$

where τ is the iteration index, $\mu_{i,\beta}$, $\mu_{i,\rho}(\tau)$ are the positive decreasing step rules are satisfied, the solution of the power allocation optimization problem converges to an optimal solution. The algorithm is summarized next.

Algorithm 1: Scheduling and Power Allocation Algorithm	
Input:	Set of RBs, D2D users, p_{max}, R_i^{min}, g_{ij}, g_{kj}, γ_{th}
Output:	Capacity,R_{ij} , Optimal transmit power, p_{ij}^*
Define	Iteration number $m = 1$, p_{ij}, iteration tolerance $\varepsilon > 0$, $\mu_{i,\beta} = 0.001$, $\mu_{i,\rho} = 0.001$, M, β_i, ρ_i
Initialize	$\mathbb{B} = \phi$,

	for $i \in \mathbb{U}$, $j \epsilon \mathbb{B}$,
	Compute, γ_{ij} using (4)
	if$\gamma_{ij} \geq \gamma_{th}$, then
	$\mathbb{B}_j = \mathbb{B}_j \cup \{j\}$ and
	$\mathbb{B} = \{\mathbb{B}_i | i \in \mathbb{U}\}$
	if $\mathbb{B} = 0$,
	terminate
	end if
	end if
	end for

	for $i \in \mathbb{U}$, compute $F(m)$ using (8) while $\lvert F(m)\rvert \geq \varepsilon$ or $m \leq M$**do** Compute p_{ij} using (10); If $\lvert F(m)\rvert < \varepsilon$ $p_{ij}^* = p_{ij}$ else update β_i, ρ_i using (13) and (14); $p_{ij}(m+1)$, $F(m)$

	Next iteration, $m = m + 1$
	until β_i, ρ_i converge
	end if
	end while
	end for
	return p_{ij}^*, R_{ij}

D. Resource Scheduling Algorithm

The formulated power allocation problem was combined with a Best Channel Quality Indicator (BCQI) resource scheduling algorithm. This algorithm allocates RBs to the D2D devices for best channel conditions. The mobile device generates the CQI information and feeds it to the BS periodically in a quantized form with some delay. The value of the SINR is contained in the CQI information. The best channel condition given by the highest value of the CQI information and it is the one selected for the scheduling process. The BCQI scheduling algorithm offers higher throughput than round-robin and proportional fair resource scheduling algorithms. The BCQI algorithm flow-charts is shown in Figure-1. The BCQI scheduling can mathematically be expressed as;

$$k = arg \max_{i,j} R_{ij} \quad (5)$$

where R_{ij} is the instantaneous data rate for the i$^{th}D_T$device.

©2006-2021 Asian Research Publishing Network (ARPN). All rights reserved.

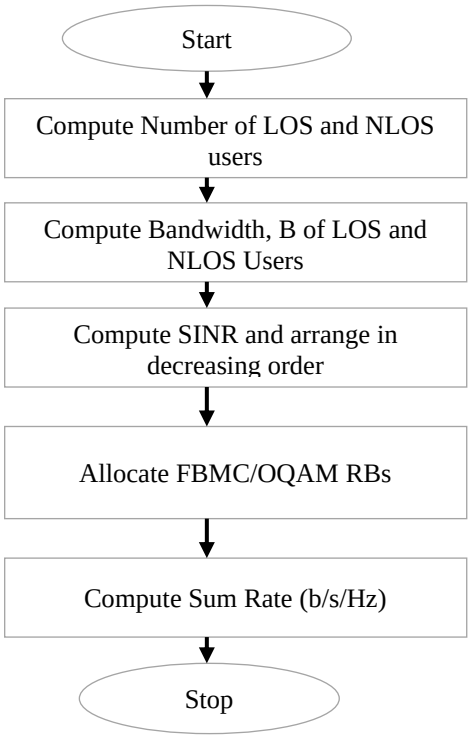

Figure-1. The BCQI Algorithm.

USER MOBILITY AND BLOCKING MODELS

The random waypoint mobility model which is widely used in the simulation of wireless mobile networks is adopted in this study. All D2D devices' have a uniformly distributed random initial positions within the cell coverage. There is a random and independent determination for device destination, the speed at which it moves, and its direction. When the user reaches its destination, it stays there for some random time duration before moving to a new position. Each user moves in a random direction within the cell with a constant speed ranging from 1-100km/h. The new device position at a given time can be given by;

$$\mathrm{d_i(t)} = \mathrm{d_i(t-1)} + [(\mathrm{v_i(t-1)} \times \mathrm{dir_i(t-1)})] \times \mathrm{t} \quad (16)$$

where $d_i(t)$ gives the location of a $D_T$device, i at time t,$v_i(t-1)$ is the speed of D_T device, i at time $t-1$and $dir_i(t-1)$ is the direction of D_T device, i at time $t-1$. The D2D devices are maintained within the cell by using a wrap-round model where the user enters the cell from the opposite edge when it has reached the cell boundaries. The study used line blocking which reduced the signal strength and the likelihood of blocking is given by;

$$p_{bl} = 1 - e^{-\lambda(x-r_{bl})r_{bl}} \quad (17)$$

where λ is the arrival rate of users, x is the x-coordinate of the $D_T$device, and r_{bl} is the radius of the blocking object.

MULTICARRIER MODULATION

A. FBMC/OQAM and OFDM

In multicarrier systems, the signal information is propagated through pulses having a time and frequency overlap. The time-domain representation of a transmitted signal in a multicarrier communication system can be given as in (15) [27];

$$s(t) = \sum_{k=0}^{K-1} \sum_{l=0}^{L-1} g_{l,k}(t) x_{l,k} \quad (18)$$

where $x_{l,k}$ is the transmitted data symbol for subcarrier point l and time point k which is selected in a QAM signal constellation, K is the total number of time positions and L is the total number of frequency positions. The basis pulse that is transmitted can be given by;

$$g_{l,k}(t) = g(t-kT)e^{j2\pi lF(t-kT)}e^{j\theta_{l,k}} \quad (19)$$

This pulse $g_{l,k}(t)$ shows the response of the prototype filter $p(t)$ which is shifted in time and frequency over a time spacing, T and frequency spacing or subcarrier spacing, F. The data symbols received at the BS are decoded by projecting the received signal, $r(t)$onto the basis pulses giving a decoded signal as;

$$y_{l,k} = < r(t), g_{l,k}(t) > = \int_{-\infty}^{\infty} r(t) g_{l,k}^{*}(t) dt \quad (20)$$

The basis pulses can be chosen differently for the transmitter and receiver as shown in [28].

B. MIMO Space-Time Coded FBMC/OQAM

The deployment of multiple antennas at the transmitter and/or receiver can improve performance in mm-wave communication to provide spatial diversity for the network. The space-time block code or the space-time trellis coding can be used to implement spatial diversity. Due to the challenge of mitigating interference in space-time trellis coding, it only works well for single time delay coding applications. The Alamouti scheme has been widely adopted in wireless networks to achieve transmit diversity with two transmit antennas and one receive antenna [29]. Then, considering a millimeter-wave communication network having N_T and N_R antennas and whose communication based on FBMC/OQAM multicarrier modulation; the output of synthesis filter bank (SFB) for transmission antennas t_a can be expressed as [30, 31];

$$s^{(t_a)}(t) = \sum_{k=0}^{K-1} \sum_{l=0}^{L-1} g_{l,k}(t) x_{l,k}^{t_a} \quad (21)$$

where (l,k) denotes subcarrier, l and FBMC symbol having a time position, $k, x_{l,k}^{t_a}$ is the real part of the OQAM symbols for an even number of the subcarriers. The prototype filter with unit energy has an impulse response, $g_{l,k}(t)$ given by (16). The prototype filter has an impulse response of length $L_g$and the phase $\varphi_{l,k}$ which can be given by;

©2006-2021 Asian Research Publishing Network (ARPN). All rights reserved.

$$\varphi_{l,k} = (l+k)\frac{\pi}{2} - lk\pi \quad (22)$$

The length of the filter usually satisfies the condition which is expressed as, $L_g = O.L$ with O being the overlapping factor. Assuming the time-invariant systems, the channel from the transmission antenna, t_a, to the receiving antenna has a frequency response expressed in matrix form as;

$$H^{(t_a,r_a)} = \left[H_0^{(t_a,r_a)} H_1^{(t_a,r_a)} \dots H_{L-1}^{(t_a,r_a)}\right]^T \quad (23)$$

The noise signal at the transmitter and receiver antennas can be assumed as a zero-mean Gaussian with a variance of σ^2 with no correlation with one another implying temporarily and spatially white noise. Assuming the low channel delay spread, the analysis filter bank (AFB) has its output at the receive antenna r_a and frequency-time point (p, q) given by (24) [30];

$$y_{p,q}^{r_a} = \sum_{t_a=1}^{N_T} H_p^{(t_a,r_a)} C_{p,q}^{t_a} + w_{p,q}^{r_a} \quad (24)$$

where $w_{p,q}^{r_a}$ is AWGN with variance σ^2 with no correlation in both time and the frequency, $C_{p,q}^{t_a}$ is the transmitted symbol which also contains the imaginary interference from its first order frequency-time neighborhood and is expressed as (25);

$$C_{p,q}^{t_a} = x_{p,q}^{t_a} + \jmath \sum_{l,k\epsilon\Omega_{p,q}} \langle g \rangle_{l,k}^{p,q} x_{l,k}^{t_a} \quad (25)$$

This can be simplified as (26);

$$C_{p,q}^{t_a} = x_{l,k}^{t_a} + ju_{l,k}^{t_a} \quad (26)$$

where $u_{l,k}^{t_a}$ is the interference term. The received signal $y_{l,k}^{r_a}$ can be expressed as (25);

$$y_{l,k}^{r_a} = H_{l,k}^{(t_a,r_a)} C_{l,k}^{t_a} + w_{l,k}^{r_a} \quad (27)$$

where $H_{l,k}^{(t_a,r_a)}$ denotes channel coefficients between the transmitter and receiver antenna at a frequency l and time instant k, $w_{l,k}^{r_a}$ denotes the noise signal received at the receiver. The MIMO systems applied in this case has N_T antennas to transmit data to N_R receive antennas of which at the frequency-time position (l,k) the received signal can be expressed as (28);

$$\begin{aligned} y_{l,k}^{r_a} &= \sum_{t_a=1}^{N_T} H_{l,k}^{(t_a,r_a)} C_{l,k}^{t_a} + w_{l,k}^{r_a} \\ &= \sum_{t_a=1}^{N_T} H_{l,k}^{(t_a,r_a)} \left(x_{l,k}^{t_a} + ju_{l,k}^{t_a}\right) + w_{l,k}^{r_a} \end{aligned} \quad (28)$$

This can be expressed in matrix form as;

$$\begin{bmatrix} y_{l,k}^{1} \\ \vdots \\ y_{l,k}^{N_R} \end{bmatrix} = \begin{bmatrix} H_{l,k}^{11} & \dots & H_{l,k}^{1N_T)} \\ \vdots & \ddots & \vdots \\ H_{l,k}^{N_R 1)} & \dots & H_{l,k}^{N_R,r_a)} \end{bmatrix} \begin{bmatrix} x_{l,k}^{t_a} & + & ju_{l,k}^{t_a} \\ \vdots & \vdots & \vdots \\ x_{l,k}^{N_T} & + & ju_{l,k}^{N_T} \end{bmatrix} + \begin{bmatrix} w_{l,k}^{1} \\ \vdots \\ w_{l,k}^{N_R} \end{bmatrix} \quad (29)$$

The capacity in bits per second for a space-time coded FBMC/OQAM can then be given by (30);

$$C = W.\log_2\left[\det\left(I_{N_R} + \frac{\rho}{N_T} H_{l,k} H_{l,k}^{*}\right)\right] \quad (30)$$

where W is the total channel bandwidth, I_{N_R} is the identity matrix with dimensions equal to the number of receive antennas.

MILLIMETER-WAVE CHANNEL MODEL

The aggregate loss of a signal during propagation through a channel is the summation of shadowing and large scale fading. The path loss experienced by the signal when undergoing transmission from the transmitter to the receiver is dependent on transmission distance. The shadowing is a deviation between the transmitter and receiver mean path loss due to the power dissipation of the signal through the transmission channel. The Line-of-Sight (LOS) and Non-Line-of-Sight (NLOS) components contribute to the total path loss experienced by the received signal. The path loss model considered in his study is the close-in reference distance model developed for mm-wave D2D communication and is given as (31) [32].

$$PL[dB] = 20\,log\frac{4\pi f}{c} + 10\alpha\,log\,d + \chi \quad (31)$$

where f denotes carrier frequency of operation in *GHz*, c is the velocity of light in a vacuum, α represents the path loss parameter, and d denotes the range between transmit and receiving device, and χ represents the shadowing standard deviation in dB.

SIMULATION AND PERFORMANCE EVALUATION

The FBMC/OQAM based mm-wave D2D communication model was simulated in MATLAB with user mobility for a single cell of radius 250m, a system bandwidth of 1GHz, 50 resource blocks in every slot and one dual-band BS of carrier frequency 28GHz. The arrival rate of D2D users varies between 1 and 12. The D2D users are randomly distributed in a circular cell by Poisson Point Process (PPP). The path loss model for the D2D user links is determined according to the NYUSIM model presented in [32, 33]. The path loss parameters were taken as; $\alpha_L = 2$ for LOS, $\alpha_N = 3$ for NLOS.

The capacity for scheduling and resource allocation for the mm-wave D2D communication network was determined for FBMC/OQAM by varying the rate at which the users enter the cell per unit time from 1 to 12.

©2006-2021 Asian Research Publishing Network (ARPN). All rights reserved.

The study considered an FBMC/OQAM with a modulation order of *I*= 64 and *I*=256 with an assumption that there is no total blockage of the signal for NLOS conditions. The parameters used in the simulation of the network are summarized in Table-1.

Table-1. Model Simulation Parameters.

Parameter Description	Notation	Value
Simulation Area	*A*	500m
Radius	*R*	250m
Transmit Power of D2D Device	P_t	20dBm
Carrier frequency	f_c	28GHz
Noise power Spectral Density (dBm)	*No*	-174
Bandwidth	*W*	1GHz
Number of Resource Blocks	*RBs*	50
Arrival Rate (users/sec)	λ	[1:12]
Modulation order	*I*	64, 256
Subcarrier spacing	*B*	15kHz
No. of antennas at RX	N_R	4
No. of antennas at TX	N_T	4
User Velocity	*v*	8km/h
No. of subcarriers	N_f	12
Total number of symbols	*Ns*	30
Overlapping factor	*O*	4 & 8

Both LOS and NLOS users were considered in this study. The users were distributed randomly by the Poisson Point Process with the arrival rate varying from 1 to 12 per unit time. The users' positions were updated by the equations in (32);

$$x_n = x_{n-1} + d\cos\theta \qquad (32)$$
$$y_n = y_{n-1} + d\sin\theta$$

Since distance is given by the product of user mobility velocity and time, then the update equations may be re-written as;

$$x_n = x_{n-1} + v.t\cos\theta \qquad (33)$$
$$y_n = y_{n-1} + v.t\sin\theta$$

where v is the velocity at which the user moves in km/hr and θ is the angle between transmitter and receiver device., both randomly selected for each user.

A. Scheduling for Equal Power Allocation

The simulation results for scheduling and resource allocation incorporating the best channel quality indicator algorithm in mm-wave D2D communication with user mobility are given. Figure-2 shows the capacity of multicarrier modulation (FBMC/OQAM) against the arrival rate of users for D2D-enabled mm-wave multicarrier communication for LOS and NLOS with user mobility taken into consideration for a modulation order of *I*=64. It shows the capacity of LOS conditions is higher compared to the NLOS conditions. This is due to the signal blockings for NLOS conditions which degrades the signal strength.

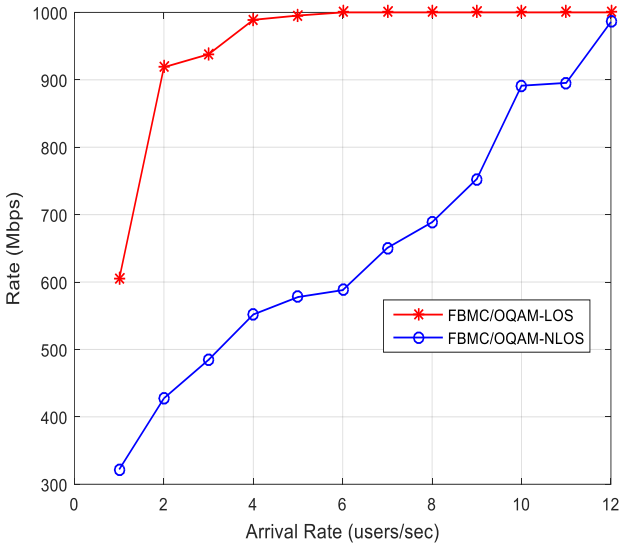

Figure-2. Capacity variation for a modulation order *I*=64 with a change in arrival rates.

Figure-3 shows the capacity variation when the modulation order is increased to *I*=256. It shows that the capacity starts at 850Mbps for an arrival rate of one user/second. The performance of LOS users is still better compared to NLOS users which is consistent with that of modulation order was *I*=64.

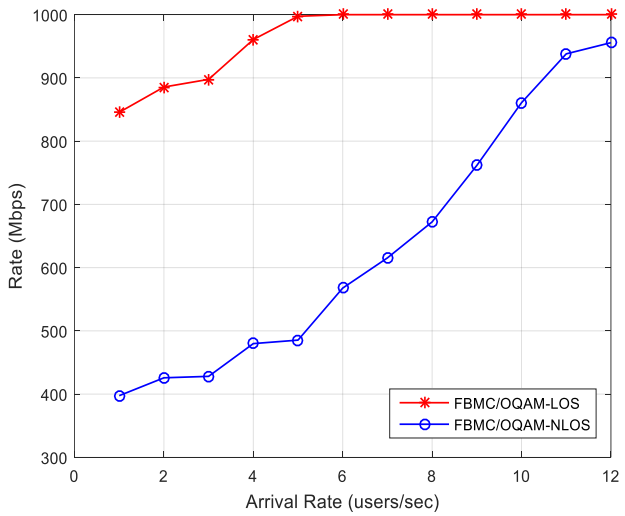

Figure-3. Capacity variation for a modulation order *I=256* with a change in arrival rates.

Figure-4 shows the comparison of performance for modulation orders of 64 and 256. For the arrival rate of between 1-5 users per second the FBMC/OQAM with a modulation order of 64 performs better compared with the modulation order of *I*=256 for LOS conditions. After the

©2006-2021 Asian Research Publishing Network (ARPN). All rights reserved.

arrival rate of 5 users/sec, the capacity for LOS remains constant at 1000Mbps which is the highest capacity attainable for a bandwidth of 1GHz according to Shannon's theorem.

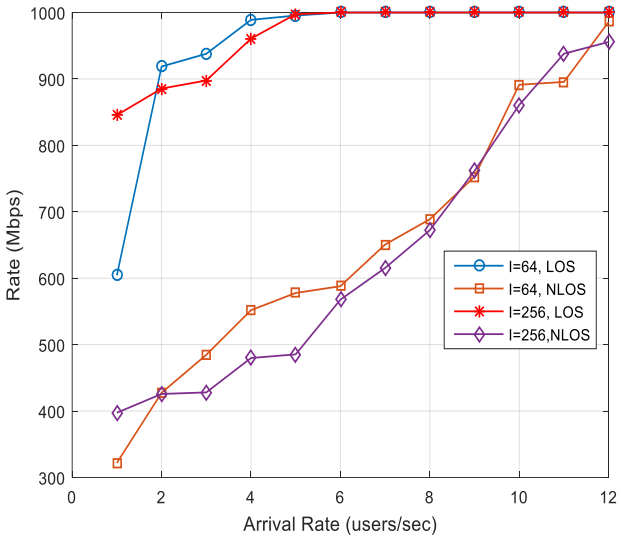

Figure-4. Comparison of capacity FBMC/OQAM with I=64 and I=256.

Figure-5 shows the variation of the capacity of the OFDM multicarrier communication scheme with user mobility for LOS and NLOS conditions. The LOS scenario performs better than the NLOS case since the signal blockings degrade the received signal strength.

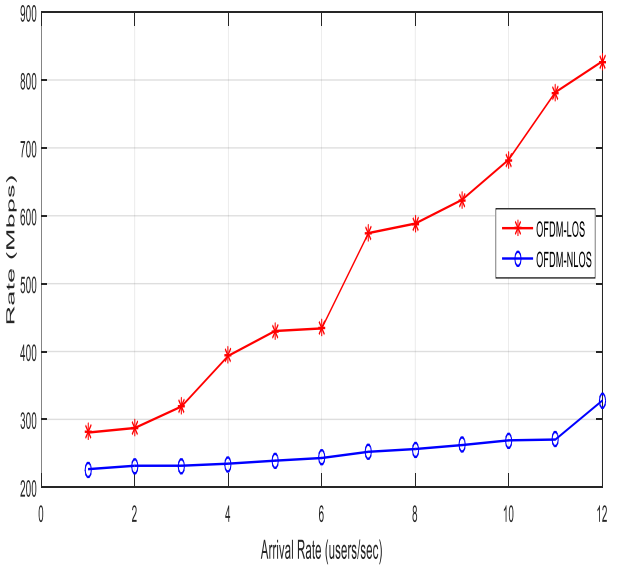

Figure-5. Capacity variation for OFDM modulation with the change in arrival rates.

The evaluation and demonstration of the effectiveness of the proposed algorithm have been given by comparing the FBMC/OQAM based communication with the conventional OFDM as shown in Figure-6 for line-of-sight cases. It is seen that the FBMC/OQAM performs better both LOS and NLOS cases compared to the OFDM scheme in terms of capacity in D2D enabled mm-wave multicarrier communication network with user mobility.

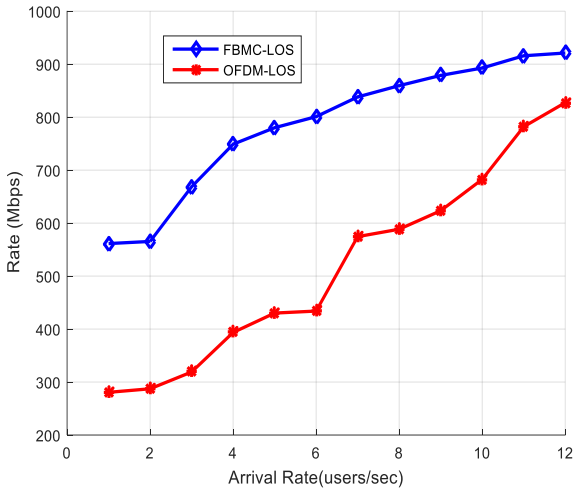

Figure-6. Comparison of FBMC-OQAM and OFDM Modulation for LOS.

Figure-7 shows the comparison of capacity for FBMC/OQAM and OFDM for the NLOS case. It can be seen also that the capacity is better in FBMC/OQAM than the OFDM scheme. This makes the FBMC/OQAM modulation scheme a more suitable candidate to handle the future data capacity which is projected to be very high.

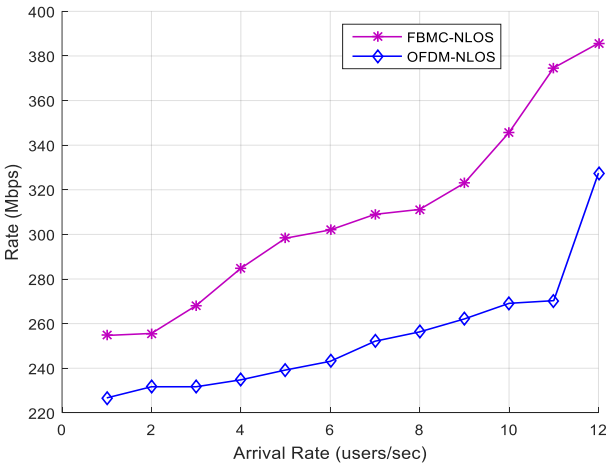

Figure-7. Comparison of capacity variation for FBMC-OQAM and OFDM for NLOS with the change in arrival rates.

B. Scheduling for Space-Time Coded and Spatial Multiplexing Transmission

Figure-8 shows the capacity of the D2D user devices when the Alamouti 2×1 diversity scheme with modulation order I=64 considered for FBMC/OQAM. The results show that the Alamouti 2×1 scheme improves the capacity for LOS users which is almost similar to the

©2006-2021 Asian Research Publishing Network (ARPN). All rights reserved.

result obtained when the modulation order is *I*=256. This implies transmit diversity incorporation for scheduling and resource allocation process in D2D communication in cellular mode can greatly improve performance.

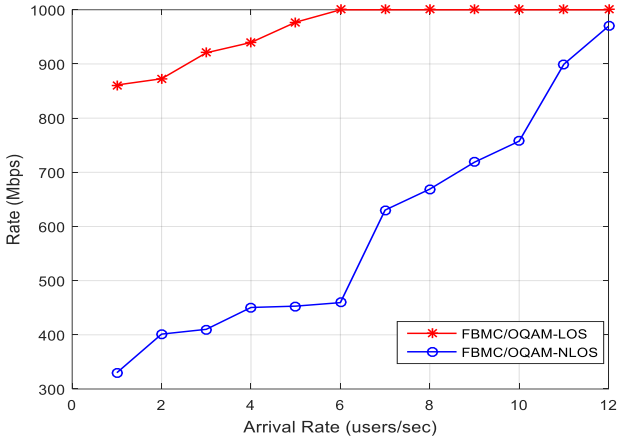

Figure-8. Alamouti space-time block coding for FBMC/OQAM.

Figure-9 shows the throughput attained by incorporating spatial multiplexing with FBMC/OQAM multicarrier modulation for mm-wave D2D communication. In this case spatial multiplexing with maximum likelihood equalization is applied when there is no requirement for perfect CSI. It can be shown that spatially multiplexed FBMC/OQAM has a better performance for LOS compared to NLOS conditions.

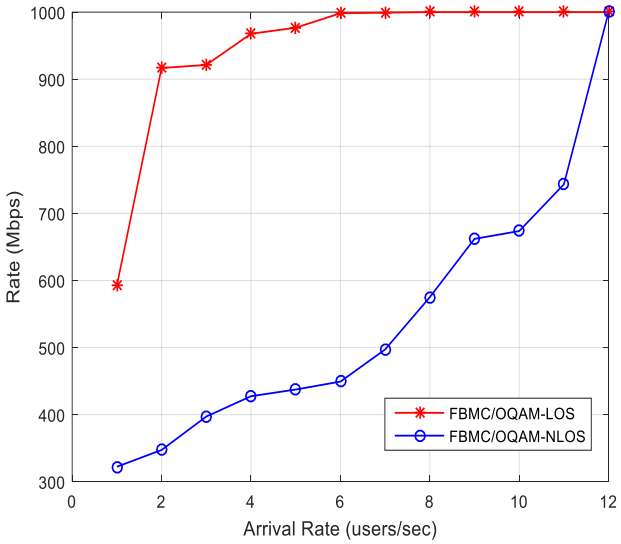

Figure-9. Spatially multiplexed FBMC/OQAM modulation.

Figure-10 shows the capacity for spatial multiplexing with maximum likelihood equalization when perfect channel state information is required. It was shown the capacity of D2D devices was degraded when there was a requirement for perfect channel knowledge.

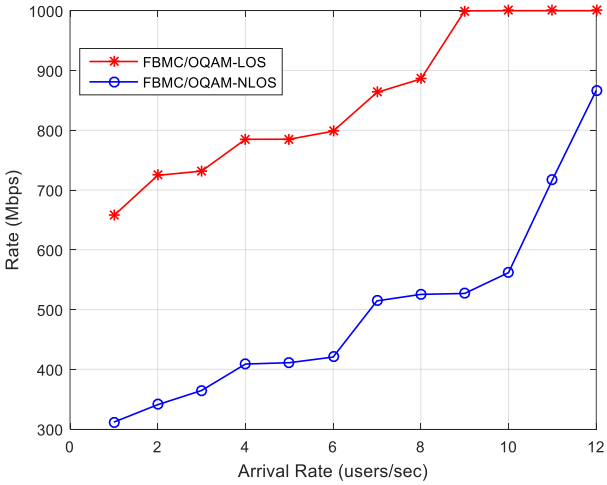

Figure-10. Spatially-multiplexed FBMC/OQAM with perfect CSI.

The comparison of the variation of capacity for FBMC/OQAM modulation with the change of I-ary modulation order and arrival rates is given in Figure-11. The results show that space-time coded (STC) FBMC/OQAM modulation produced almost the same result as that of *I*=256 but lower than that of *I*=64for the LOS scenario. However, in NLOS scenario FBMC/OQAM with *I*=64 offers the best result, followed by that of *I*=256 and finally space-time block coded FBMC/OQAM. Therefore, it can be concluded that the space-time block coded FBMC/OQAM can be implemented only in LOS scenarios other than increasing the modulation order.

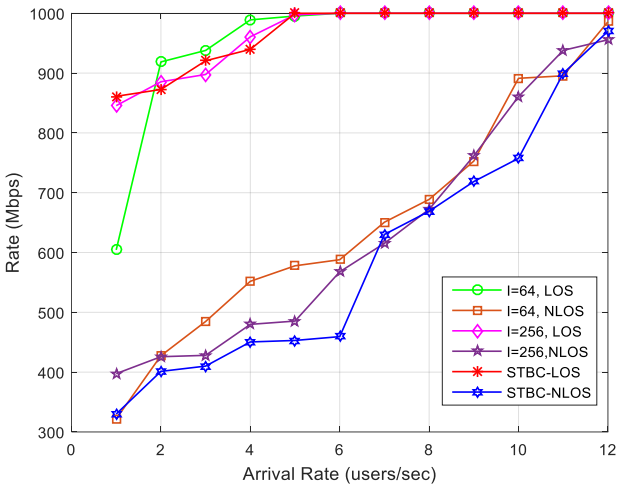

Figure-11. Comparison of capacity for I=64, I=256 and STBC-FBMC/OQAM.

The comparison of iterative water-filling power allocation and equal power allocation algorithms is given in Figure-12. The result shows that the iterative water-filling algorithm can enhance performance in terms of capacity unlike when scheduling is done with an assumption of equal power allocation. Since the BCQI algorithm performs poorly in terms of fairness, the water

©2006-2021 Asian Research Publishing Network (ARPN). All rights reserved.

filling algorithm can mitigate this by ensuring fairness in power allocation.

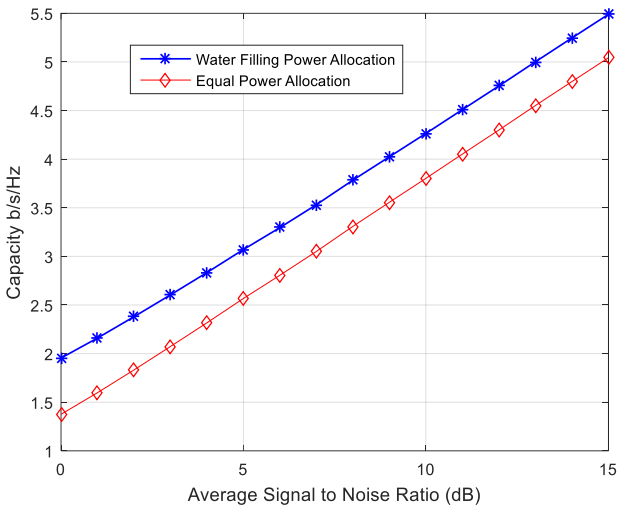

Figure-12. Comparison of iterative water filling and equal power allocation algorithms.

CONCLUSIONS

The paper has studied a combined scheduling and power allocation problem for a D2D-enabled millimeter-wave multicarrier communication network in cellular mode with user mobility. The FBMC/OQAM multicarrier modulation scheme was integrated to the scheduling and power allocation optimization problem to maximize the capacity of D2D user devices by applying the BCQI algorithm. The results showed the performance of joint scheduling and power allocation based on FBMC/OQAM multicarrier modulation outperformed that of OFDM/QAM modulation. The FBMC/OQAM performance better by an average factor of 2.03 times for *I*=64, LOS, 2.53 times for *I*=64, NLOS, 2.08 times for *I*=256, LOS, 2.45 times for *I*=256, NLOS, 2.08 times for STC, LOS and 2.30 times for STC, NLOS compared to that ofOFDM/QAM. It was also shown that space-time coding offers a performance for LOS conditions which is 1.786 times that for NLOS conditions. The comparison of *I*=64 and *I*=256 modulation order shows that space-time coding can be implemented for LOS conditions due to its poor performance in the NLOS case. The iterative water-filling power allocation algorithm provided higher performance than equal power allocation. The LOS results showed a better performance compared to the NLOS network scenario for all the cases that were considered due to the presence of blockage for the NLOS case. The study can be extended to D2D reuse mode by considering the effect of interference originating from D2D pairs on the cellular user performance when both are implemented in the millimeter-wave band with user mobility.

ACKNOWLEDGMENT

The work was supported by Pan African University Institute for Basic Sciences, Technology and Innovation.

REFERENCES

[1] S. El Hassani, A. Haidine and H. Jebbar. 2019. Road to 5G: Key Enabling Technologies. Journal of Communications, 14(11): 1034-1048.

[2] T. S. Rappaport, G. R. MacCartney, M. K. Samimi and S. Sun. 2015. Wideband Millimeter-Wave Propagation Measurements and Channel Models for Future Wireless Communication. IEEE Transactions on Communications. 63(9): 3029-3056.

[3] G. R. MacCartney, T. S. Rappaport, S. Sun and S. Deng. 2015. Indoor Office Wideband Millimeter-Wave Propagation Measurements and Channel Models at 28 and 73GHz for Ultra-dense 5G Wireless Networks. IEEE Access. 3: 2388-2424.

[4] B. P. Sahoo, C. H. Yao and H. Y. Wei. 2017. Millimeter-Wave Multi-hop Wireless Backhauling for 5G Cellular Networks. in 85th IEEE Vehicular Technology Conference, Sydney, Australia.

[5] X. Song, X. Han and S. Xu. 2019. Joint Power Control and Channel Assignment in D2D Communication System. Journal of Communications. 14(5): 349-355.

[6] S. Chen, S. Sun, Q. Gao and X. Su. 2016. Adaptive Beamforming in TDD-based Mobile Communication Systems: State of the Art and 5G Research. IEEE Wireless Communications. 23(6): 81-87.

[7] S. Kutty and D. Sen. 2016. Beamforming for Millimeter Wave Communications: An Inclusive Survey. IEEE Communication Surveys and Tutorials. 18(2): 949-973.

[8] A. C. Honfoga, T. T. Nguyen, M. Dossou and V. Moeyaert. 2019. Application of FBMC to DVB-T2: A Comparison vs Classical OFDM Transmissions. in IEEE Global Conference on Signal and Information Processing, Ottawa, Canada.

[9] E. Kofidis and V. Dalakas. 2019. Filter Bank-based Multiple Access in Next Generation Satellite Uplinks: A DVB-RVCS2-based Experimental Study. in 2nd IEEE 5G World Forum, Dresden, Germany.

[10] V. Dalakas and E. Kofidis. 2020. Filter Bank-based Multiple Access in Next Generation Satellite Uplinks: A DVB-RCS2-based Experimental Study. International Journal of Satellite Communications and Networking. pp. 1-12.

©2006-2021 Asian Research Publishing Network (ARPN). All rights reserved.

[11] C. Sexton, Q. Bodinier, A. Farhang, N. Marchetti, F. Bader and L. A. Dasilva. 2016. Coexistence of OFDM and FBMC for underlay D2D Communication in 5G Networks. in IEEE Globecom, Washington, USA.

[12] M. Renfors, X. Mestre, E. Kofidis and F. Bader. 2017. Academic Press.

[13] G. Femenias, F. Riera-Palou, X. Mestre and J. J. Olmos. 2017. Downlink Scheduling and Resource Allocation for 5G MIMO-Multicarrier: OFDM vs FBMC/OQAM. IEEE Access. 5: 13770-13786.

[14] A. Vora and K. D. Ang. 2018. Downlink Scheduling and Resource Allocation for 5G MIMO-Multicarrier Systems. in IEEE 5G World Forum (5GWF), Dresden, Germany.

[15] P. S. Bithas, K. Maliatsos and F. Foukalas. 2019. An SINR Joint Mode Selection, Scheduling and Resource Allocation Scheme for D2D Communications. IEEE Transactions on Vehicular Technology. 68(5): 4949-4963.

[16] C. Sexton, Q. Bodinier, A. Farhang, N. Marcheti, F. Bader and L. A. DaSilva. 2018. Enabling Asynchronous Machine-Type D2D Communication using Multiple Waveforms in 5G. IEEE Internet of Things Journal. 5(2): 1307-1322.

[17] A. Abrardo and M. Moretti. 2016. Distributed Power Allocation for D2D Communications underlying/ Overlaying OFDMA Cellular Networks. IEEE Transactions on Wireless Communications. 16(3): 1466-1479.

[18] C. H. Yao, C. Y. Y., B. P. Sahoo and H. Y. Wei. 2017. Outage Reduction with Joint Scheduling and Power Allocation in 5G mmWave Cellular Networks. in IEEE 28th Annual Symposium on Personal, Indoor and Mobile Radio Communications (PIMRC), Montreal, Canada.

[19] Y. Li, J. Luo, W. Xu, N. Vucic, E. Pateromichelakis and G. Caire. 2017. A Joint Scheduling and Resource Allocation Scheme for Millimeter Wave Heterogeneous Networks. in IEEE Wireless Communications an Networking Conference (WCNC), San Francsisco, USA.

[20] N. A. Priyadharsini. 2019. Effective Scheduling Policies to Optimize Radio Resources between NR-gNodeB and Device to Device Systems in 5G. Wireless Personal Communications. 109(2): 1071-1093.

[21] L. Wang, S. Liu, M. Chen, G. Gui and H. Sari. 2019. Sidelobe Interference Reduced Scheduling Algorithm for mmWave Device-to-Device Communication Networks. Peer-to-Peer Networking and Applications. 12(1): 228-240.

[22] P. Wu, P. C. Cosma and L. B. Milstein. 2016. Resource Allocation for Multicarrier Device-to-Device Video Transmission: Symbol Error Rate Analysis and Algorithm Design. IEEE Transactions on Communication. 65(10): 4446-4462.

[23] O. Semiari, W. Saad and M. Bennis. 2017. Joint Millimeter Wave and Microwave Resources Allocation in Cellular Networks with Dual-Mode Base Stations. IEEE Transactions on Wireless Communications. 16(7): 4802-4816.

[24] R. Mudumbai, S. Singh and U. Madhow. 2009. Medium Access Control for 6oGHz Outdoor Mesh Networks with Highly Directional Links. in IEEE Infocom, Rio de Janeiro, Brazil.

[25] W. Dinkelbach. 1967. On Nonlinear Fractional Programming. Management Science. 13(7): 492-498.

[26] S. Boyd and L. Vandenberghe. 2004. Convex Optimization, Cambridge University Press.

[27] R. Nissel, S. Schwarz and M. Rupp. 2017. Filter Bank Multicarrier Modulation Schemes for Future Mobile Communications. IEEE Journal on Selected Areas in Communications. 35(8): 1768-1782.

[28] G. S. D. Matz, K. Grochenig, M. Hartmann and F. Hlawatsch. 2007. Analysis, Optimization and Implementation of Low-Interference Wireless Multicarrier Systems. IEEE Transactions on Wireless Communications. 6(5): 1921-1931.

[29] S. Alamouti. 1998. A Simple Transmit Diversity Technique for Wireless Communications. IEEE Journal on Selected Areas in Communications. 16(8): 1451-1458.

[30] E. Kofidis, D. Katselis, A. Rontogiannis and S. Theodoridis. 2013. Preamble-Based Channel Estimation in OFDM/OQAM Systems: A Review. Signal Processing. 93(7): 2018-2054.

©2006-2021 Asian Research Publishing Network (ARPN). All rights reserved.

[31] B. Farhang-Boroujeny. 2011. OFDM versus Filter Bank Multicarrier. IEEE Signal Processing Magazine. 28(3): 92-116.

[32] S. Shun, R. Theodore, R. Sundeep, A. Timothy, G. Amitara, K. Istvan, R. Ignacio, K. Ozge and P. Andrezej. 2016. Propagation Path Loss Models for 5G Urban Micro and Macro-Cellular Scenarios. in IEEE 83rd Vehicular Technology Conference, Nanjing, China.

[33] S. Sun, T. S. Rappaport, M. Shafi, P. Tang, J. Zhang and P. J. Smith. 2018. Propagation Models and Performance Evaluation for 5G Millimeter-Wave Bands. IEEE Transactions on Vehicular Technology. 67(9): 8422-8439.